Numerical models for seismic analysis of arch dams

Conference Paper · September 2022

6 authors, including:


André Alegre
Instituto Politécnico de Lisboa
28 PUBLICATIONS **104** CITATIONS
SEE PROFILE


Sérgio Oliveira
National Laboratory for Civil Engineering
38 PUBLICATIONS **178** CITATIONS
SEE PROFILE


Paulo Mendes
Instituto Politécnico de Lisboa
59 PUBLICATIONS **178** CITATIONS
SEE PROFILE


Ezequiel Carvalho
Hidroelectrica de Cahora Bassa
17 PUBLICATIONS **40** CITATIONS
SEE PROFILE

Congreso de Métodos Numéricos en Ingeniería
12-14 septiembre 2022, Las Palmas de Gran Canaria, España

NUMERICAL MODELS FOR SEISMIC ANALYSIS OF ARCH DAMS

André Alegre[1,2], Sérgio Oliveira[2], Paulo Mendes[1], Jorge Proença[3], Ezequiel Carvalho[4] and Bruno Matsinhe[4]

1: Civil Engineering Department
Instituto Superior de Engenharia de Lisboa (ISEL), Instituto Politécnico de Lisboa (IPL)
Rua Conselheiro Emídio Navarro 1, Lisboa, Portugal
e-mail: andrefalegre92@gmail.com, pmendes@dec.isel.ipl.pt, web: http://www.isel.pt

2: Concrete Dams Department
National Laboratory for Civil Engineering (LNEC)
Av. do Brasil 101, 1700-075 Lisboa, Portugal
e-mail: soliveira@lnec.pt, web: http://www.lnec.pt

3: Department of Civil Engineering, Architecture and Georesources (CERIS)
Instituto Superior Técnico (IST), Universidade de Lisboa (ULisboa)
Av. Rovisco Pais 1, Lisboa, Portugal
e-mail: jorge.m.proenca@tecnico.ulisboa.pt, web: http://tecnico.ulisboa.pt

4: Hidroelétrica de Cahora Bassa (HCB)
Office Headquarters
Songo, Maputo, Mozambique
e-mail: ezequiel.carvalho@hcb.co.mz, bruno.matsinhe@hcb.co.mz, web: https://www.hcb.co.mz/

Keywords: Finite elements, seismic analysis, arch dams, joint movements, concrete damage

Abstract: *This paper presents a study on the seismic behaviour of large arch dams under strong earthquakes. The numerical simulations are carried out using DamDySSA, a 3D finite element program developed for dynamic analysis of concrete dams, which includes calculation modules for linear seismic analysis and for non-linear seismic analysis, considering the effects of joint movements and tensile and compressive damage in concrete. The case studies are the 132 m-high Cabril dam, in Portugal, and the 170 m-high Cahora Bassa dam, in Mozambique. The seismic response results computed using linear and non-linear models are compared, in order to investigate the influence of the joint movements on the structural response, and to analyse the resulting concrete damage under a strong seismic load. Overall, there was a release of arch stresses in the upper part of both dams, due to the opening of the vertical joints, and consequently an increase of vertical stresses along the main cantilevers, causing concrete tensile failure. Furthermore, this study emphasized the potential of the developed numerical methods and thus of DamDySSA for predicting the non-linear seismic behaviour of arch dams.*

1. INTRODUCTION

Large concrete dams are civil engineering structures that play a key role in the management of freshwater resources. Usually, these are structures associated with a high potential risk, since incidents or accidents can result in significant losses for populations and the environment [1]. As such, dam engineers should work towards achieving the best operational and overall safety conditions for large concrete dams. With that goal, the structural safety of dams must be ensured from the construction phase to the end of the useful life, for any scenarios involving static and dynamic loads, namely under seismic actions. In addition, the seismic hazard has been recognized as a multi-hazard [2], given that strong earthquakes can induce not only significant ground motion and thus high amplitude vibrations in the dam, but also movements along faults or discontinuities in the footprint of the dam or of the reservoir, mass movements in the surrounding areas or into the reservoir.

This is a particularly relevant subject in dam engineering, considering that many of the large concrete dams currently in operation, some of which were built several decades ago and present deterioration problems, are located in seismic zones, and that there is a great number of dams currently under construction or at the planning stages in high seismicity regions [3]. Therefore, besides investing in the permanent monitoring of dam structural health based on vibrations measured under ambient/operational excitations, e.g., using damage detection methods, it is fundamental to monitor dam behaviour before, during, and after earthquake events, namely by comparing the measured seismic response with the response calculated using numerical models, as well as to perform seismic behaviour prediction studies for evaluating common service scenarios and/or failure scenarios, in particular for seismic safety assessment under strong earthquakes [4]. In this context, it is worth emphasizing the need to develop efficient, advanced numerical models to enable a realistic prediction of the linear and non-linear seismic response of large concrete dams.

In this work, the finite element program *DamDySSA*, developed for dynamic analysis of concrete dams, is presented, and the implemented methods for linear and non-linear seismic analysis are described. Then, seismic analysis results are presented for two large arch dams, namely Cabril dam (132 m high) and Cahora Bassa dam (170 m high). For both dams, a comparison is made between linear and non-linear seismic response, in order to investigate the influence of joint movements on the principal stresses and to evaluate the resulting concrete damage under a strong, intensifying earthquake.

2. DYNAMIC MODELLING OF DAM-RESERVOIR-FOUNDATION SYSTEMS

Large concrete dams are structures of considerable size, usually with a unique and complex geometry. These dams have several discontinuities, including construction joints or cracks that may arise due to design flaws, evolutive deterioration, or strong earthquakes. Furthermore, the dynamic behaviour of dams is strongly influenced by dynamic interaction phenomena [5], namely dam-water and dam-foundation interaction. As such, for dynamic behaviour modelling, it is necessary to use models of the complete dam-reservoir-foundation system, considering the specific features of the dam and the dynamic interaction effects.

Regarding dam-reservoir dynamic interaction, there are the classic added water mass models,

using displacement-based formulations for the dam/foundation and assuming the reservoir mass effect based on the solution proposed by Westergaard [6], and the coupled models, using finite element formulations for the dam-reservoir-foundation system and considering dam-water interaction and reservoir pressure wave propagation [7]. As for foundation behaviour, there is the massless foundation approach [8], assuming the dam is supported by a deformable foundation block with a rigid boundary at the base, and the energy dissipating models, considering the foundation mass to simulate wave propagation and radiation effects [9,10].
In what concerns the seismic behaviour of arch dams, for low intensity earthquakes, usually recorded on dams [11,12], the numerical simulations can be carried out assuming linear-elastic behaviour for concrete and considering that joints in the dam body remain closed. However, under high intensity earthquakes, vibrations of greater amplitude are expected, and important deformations may occur, resulting in the opening of the vertical contraction joints [13,14], and, simultaneously, in the occurrence of high tensions and compressions, which can cause tensile and compressive concrete damage [15,16]. So, the numerical models used to predict the non-linear seismic response of arch dams should allow to simulate both the effects due to the opening/closing and sliding joint movements and the behaviour of concrete up to failure under tension and compression [17], as in the program presented in this paper.

3. FINITE ELEMENT PROGRAM FOR DYNAMIC ANALYSIS OF CONCRETE DAMS: DAMDYSSA

The numerical simulations are carried out in this work using *DamDySSA*, a 3D finite element program developed in LNEC for dynamic analysis of concrete dam-reservoir-foundation systems and optimized for studying arch dams (Figure 1). The latest version of the program includes calculation modules for modal analysis, linear seismic analysis, and non-linear seismic analysis [17]. The adopted coupled model of the dam-reservoir-foundation system and the implemented numerical methods for seismic response analysis are described next.

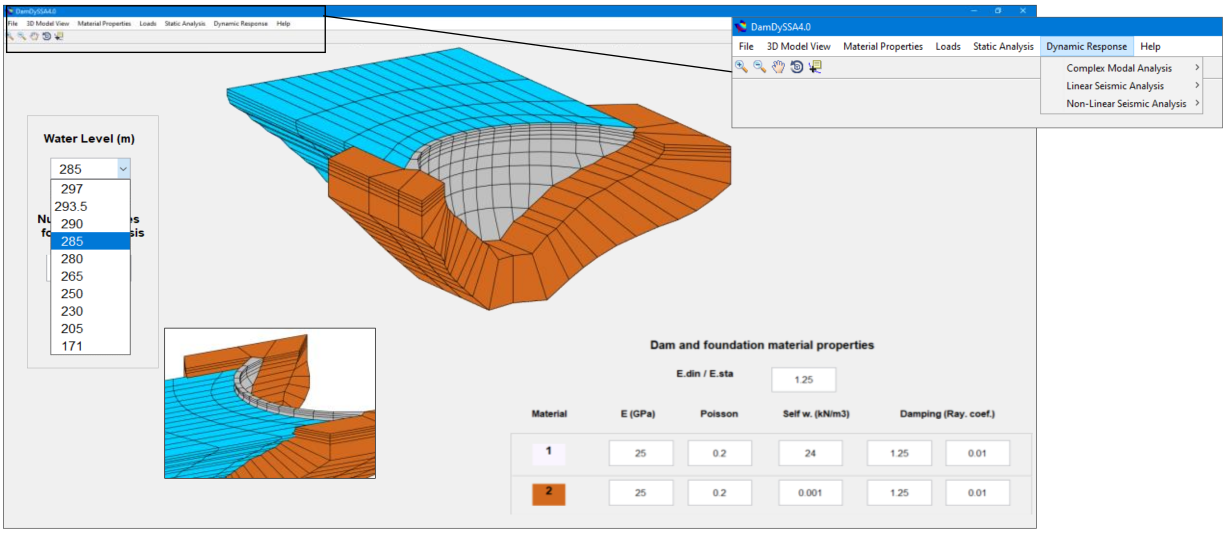

Figure 1. *DamDySSA*: a finite element program for dynamic analysis of concrete dams.

3.1. Coupled model. Dynamic behaviour of the dam-reservoir-foundation system

A coupled model is considered for simulating the dynamic behaviour of the dam-reservoir-foundation system [7,18]. The model is based on a finite element formulation in displacements (dam and foundation) and hydrodynamic pressures (reservoir). Specific boundary conditions are prescribed at the main interfaces of the solid-fluid system, in order to consider dam-water dynamic interaction, the propagation of pressure waves in the reservoir, and the reservoir free surface effect. Generalized damping is assumed, with natural viscous damping in the solid domain and energy dissipation due to radiation in the reservoir domain. The finite element equation of the discretized dam-reservoir-foundation system is defined as

$$\begin{bmatrix} \underline{m} & \underline{0} \\ \rho_w \underline{Q}^T & \underline{S} \end{bmatrix} \begin{bmatrix} \ddot{\underset{\sim}{u}} \\ \ddot{\underset{\sim}{p}} \end{bmatrix} + \begin{bmatrix} \underline{c} & \underline{0} \\ \underline{0} & \underline{R} \end{bmatrix} \begin{bmatrix} \dot{\underset{\sim}{u}} \\ \dot{\underset{\sim}{p}} \end{bmatrix} + \begin{bmatrix} \underline{k} & -\underline{Q} \\ \underline{0} & \underline{H} \end{bmatrix} \begin{bmatrix} \underset{\sim}{u} \\ \underset{\sim}{p} \end{bmatrix} = \begin{bmatrix} \underset{\sim}{F}_s \\ \underset{\sim}{F}_w \end{bmatrix} \tag{1}$$

where $\underset{\sim}{u} = \underset{\sim}{u}(t)$ is the displacements vector for the dam-foundation domain (three degrees of freedom for each node) and $\underset{\sim}{p} = \underset{\sim}{p}(t)$ is the hydrodynamic pressures vector for the reservoir domain (single pressure value for each nodal point). The mass, damping and stiffness matrices for the dam-foundation domain are $\underline{m}$, $\underline{c}$ and $\underline{k}$, while the corresponding terms for the reservoir domain are given by $\underline{S}$, $\underline{R}$ and $\underline{H}$. The coupling matrix for water-structure motion coupling is $\underline{Q}$.

The nodal force vectors in the solid and fluid domain are represented by $\underset{\sim}{F}_s = \underset{\sim}{F}_s(t)$ and $\underset{\sim}{F}_w = \underset{\sim}{F}_w(t)$, respectively; for example, the forces in the dam may include the dam self-weight, the hydrostatic pressure on the upstream face, and forces due to dynamic loads. For seismic analysis, and omitting other excitation sources, the nodal force vectors become $\underset{\sim}{F}_s = -\underline{m}\ \underline{s}\ \underset{\sim}{a}_S$ and $\underset{\sim}{F}_w = -\rho_w\ \underline{Q}^T\ \underline{s}\ \underset{\sim}{a}_S$, where $\underset{\sim}{a}_S = \underset{\sim}{a}_S(t)$ represents the seismic input, with three acceleration time histories in the upstream-downstream, cross-valley, and vertical directions, and $\underline{s}$ is a matrix to uniformly distribute the seismic accelerations by all degrees of freedom.

The substructure method is used to model the foundation block as an elastic and massless substructure, considering equivalent stiffness and damping components incorporated in the dam-rock interface. Consequently, the seismic input is uniform ground motion, applied directly at the dam base.

A true coupled approach is adopted for solving the coupled dynamic problem, without separating the solid and fluid domain equations [17]. Thus, the discrete dynamic equation of the dam-reservoir-foundation system with generalized damping is simply written

$$\underline{M}\ \ddot{\underset{\sim}{q}} + \underline{C}\ \dot{\underset{\sim}{q}} + \underline{K}\ \underset{\sim}{q} = \underset{\sim}{F} \quad , \quad \underset{\sim}{q} = \underset{\sim}{q}(t) = \begin{bmatrix} \underset{\sim}{u} \\ \underset{\sim}{p} \end{bmatrix} \tag{2}$$

where $\underline{M}$, $\underline{C}$ and $\underline{K}$ are the global mass, damping and stiffness matrices, $\underset{\sim}{F} = \underset{\sim}{F}(t)$ is the global nodal force vector, and $\underset{\sim}{q} = \underset{\sim}{q}(t)$ is the coupled unknown vector.

In *DamDySSA*, the dam-reservoir-foundation system is discretized using solid hexahedral finite elements with 20 nodes; these are isoparametric elements with 2nd degree interpolation functions, which are integrated using 27 Gauss points. The main discontinuities, e.g., dam-foundation interface, vertical contraction joints, and cracks, are discretized using compatible interface elements with 16 nodes, considering 9 integration Gauss points (Figure 2).

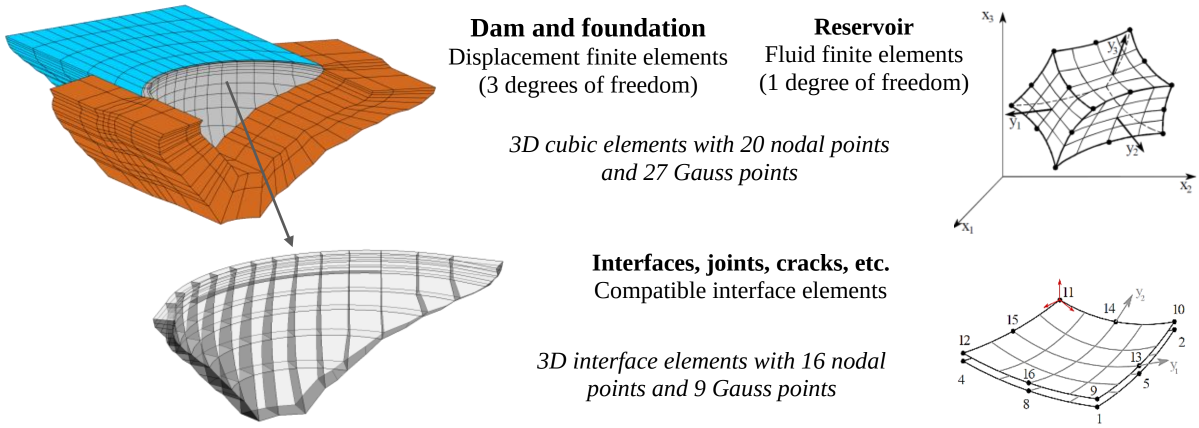

Figure 2. Discretized dam-reservoir-foundation system and used finite elements.

3.2 Time-stepping method for linear seismic analysis

The linear dynamic response of the dam-reservoir-foundation system is calculated using a time-stepping method based on the Newmark method. This formulation directly solves the coupled dynamic equation in time domain, which is defined at each time step t+Δt as

$$\underline{\mathrm{M}}\,\underset{\sim}{\ddot{\mathrm{q}}}_{\mathrm{t+\Delta t}} + \underline{\mathrm{C}}\,\underset{\sim}{\dot{\mathrm{q}}}_{\mathrm{t+\Delta t}} + \underline{\mathrm{K}}\,\underset{\sim}{\mathrm{q}}_{\mathrm{t+\Delta t}} = \underset{\sim}{F}_{\mathrm{t+\Delta t}} \tag{3}$$

For seismic analysis, in addition to the static forces due to self-weight and hydrostatic pressures, the nodal force vector $\underset{\sim}{F}_{\mathrm{t+\Delta t}}$ includes the inertia terms induced by the seismic load in the dam $\underset{\sim}{F}_{s,\mathrm{t+\Delta t}} = -\underline{\mathrm{m}}\ \underline{s}\ \underset{\sim}{a}_{S,\mathrm{t+\Delta t}}$ and in the reservoir $\underset{\sim}{F}_{w,\mathrm{t+\Delta t}} = -\rho_w\ \underline{\mathrm{Q}}^{\mathrm{T}}\ \underline{s}\ \underset{\sim}{a}_{S,\mathrm{t+\Delta t}}$.
The implemented time-stepping formulation follows the fundamentals of the original Newmark method, where the solutions for displacements and velocities are obtained from Taylor series expansions, while the accelerations are assumed to vary linearly within each time step. Application of the same principles to the coupled formulation enables the definition of approximate solutions for the coupled unknown $\underset{\sim}{\mathrm{q}} = \underset{\sim}{\mathrm{q}}(t)$ and the respective velocities $\underset{\sim}{\dot{\mathrm{q}}} = \underset{\sim}{\dot{\mathrm{q}}}(t)$, as follows

$$\begin{aligned} \underset{\sim}{\mathrm{q}}_{\mathrm{t+\Delta t}} &= \underset{\sim}{\mathrm{q}}_{\mathrm{t}} + \Delta \mathrm{t}\,\underset{\sim}{\dot{\mathrm{q}}}_{\mathrm{t}} + \Delta \mathrm{t}^2 (\frac{1}{2} - \beta)\,\underset{\sim}{\ddot{\mathrm{q}}}_{\mathrm{t}} + \Delta \mathrm{t}^2 \beta\,\underset{\sim}{\ddot{\mathrm{q}}}_{\mathrm{t+\Delta t}} \\ \underset{\sim}{\dot{\mathrm{q}}}_{\mathrm{t+\Delta t}} &= \underset{\sim}{\dot{\mathrm{q}}}_{\mathrm{t}} + \Delta \mathrm{t}\,(1-\gamma)\,\underset{\sim}{\ddot{\mathrm{q}}}_{\mathrm{t}} + \Delta \mathrm{t}\,\gamma\,\underset{\sim}{\ddot{\mathrm{q}}}_{\mathrm{t+\Delta t}} \end{aligned} \tag{4}$$

where β and γ are Newmark parameters that give the weighting contributions of the coupled accelerations at the beginning and at the end of the time interval in $\underset{\sim}{\mathrm{q}}_{\mathrm{t+\Delta t}}$ and $\underset{\sim}{\dot{\mathrm{q}}}_{\mathrm{t+\Delta t}}$.

Considering the problem expressed in terms of the coupled unknown $\underset{\sim}{\mathrm{q}}_{\mathrm{t+\Delta t}}$, and gathering terms on the left and right sides of the equation (3), results in the definition of the equivalent

‘’stiffness’’ matrix and force vector

$$\underline{K}^* = \alpha_0 \underline{M} + \alpha_1 \underline{C} + \underline{K}$$
$$\underset{\sim}{P}^*_{t+\Delta t} = \underset{\sim}{F}_{t+\Delta t} + \underline{M}\left(\alpha_0 \underset{\sim}{q}_t + \alpha_2 \dot{\underset{\sim}{q}}_t + \alpha_3 \ddot{\underset{\sim}{q}}_t\right) + \underline{C}\left(\alpha_1 \underset{\sim}{q}_t + \alpha_4 \dot{\underset{\sim}{q}}_t + \alpha_5 \ddot{\underset{\sim}{q}}_t\right) \tag{5}$$

where α_i are auxiliary constants defined by Newmark. Finally, the equivalent coupled dynamic equation of the discretized dam-reservoir-foundation system is given by

$$\underline{K}^* \underset{\sim}{q}_{t+\Delta t} = \underset{\sim}{P}^*_{t+\Delta t} \tag{6}$$

which is solved at each time step t+Δt to get the response in displacements and pressures.

3.3 Time-stepping stress-transfer method for non-linear seismic analysis

The non-linear seismic response of the arch dam-reservoir-foundation system is computed using a non-linear time-stepping stress-transfer method. Essentially, this method combines the previous time-stepping formulation with a non-linear iterative procedure to simulate non-linear dam behaviour within each time step, using constitutive models for opening/closing and sliding joint movements and for tensile and compressive concrete damage.
The non-linear dam behaviour is reproduced based on the Modified Newton’s iterative method [19], also referred to as stress-transfer or initial-stress method: the linear-elastic dam stiffness matrix is computed a priori and used throughout the entire non-linear dynamic calculation process; simultaneously, the loads are increased by applying fictitious forces on the dam, to reproduce the unbalanced stresses redistribution process that occurs due to non-linear behaviour. Therefore, a vector of unbalanced nodal forces $\underset{\sim}{\Psi}$ is introduced, and the non-linear coupled dynamic equation of the dam-reservoir-foundation system becomes

$$\underline{M}\,\ddot{\underset{\sim}{q}} + \underline{C}\,\dot{\underset{\sim}{q}} + \underline{K}\,\underset{\sim}{q} = \underset{\sim}{F} + \underset{\sim}{\Psi} \tag{7}$$

Following the time-stepping procedure based on the Newmark method described in 3.2, the non-linear dynamic equation is defined at each time step t+Δt as

$$\underline{M}\,\ddot{\underset{\sim}{q}}_{t+\Delta t} + \underline{C}\,\dot{\underset{\sim}{q}}_{t+\Delta t} + \underline{K}\,\underset{\sim}{q}_{t+\Delta t} = \underset{\sim}{F}_{t+\Delta t} + \underset{\sim}{\Psi}_{t+\Delta t} \tag{8}$$

and it can be simply expressed using the equivalent form

$$\underline{K}^* \underset{\sim}{q}_{t+\Delta t} = \underset{\sim}{P}^*_{t+\Delta t} + \underset{\sim}{\Psi}_{t+\Delta t} \tag{9}$$

The equivalent global stiffness and nodal force vector are the same as in eq. (5), while $\underset{\sim}{\Psi}_{t+\Delta t}$ is the vector containing the unbalanced forces computed in the stress-transfer process.

Stress-transfer process

The stress-transfer iterative process is conducted within each time step t+Δt. This process leads to the calculation of the referred unbalanced nodal forces $\underset{\sim}{\Psi}_{t+\Delta t}$, which result from the sum of the partial terms calculated in each iteration n, $\underset{\sim}{\Psi}_{t+\Delta t} = \sum \underset{\sim}{\Psi}_n$. In practice, for simulating non-linear dam behaviour, the stress-transfer process is divided into two iterative sub-processes, which are performed consecutively: the first, to simulate the effects due to joint movements, and the second, to model the concrete behaviour up to failure. Therefore, the partial unbalanced forces in every iteration n are given by

$$\underset{\sim}{\Psi}_n = \begin{bmatrix} \underset{\sim}{\Psi}_J + \underset{\sim}{\Psi}_C \\ \underset{\sim}{0} \end{bmatrix}_n \tag{10}$$

where $\underset{\sim}{\Psi}_J$ and $\underset{\sim}{\Psi}_C$ are the nodal forces associated with the unbalanced stresses due to joint and concrete non-linear behaviour, respectively. The unbalanced stresses are computed as the difference between the installed stresses and the material strength, based on the constitutive models described next.

Constitutive model for non-linear joint behaviour

The non-linear behaviour of joints is simulated using a constitutive model based on the Mohr-Coulomb failure criterion, assuming that joints cannot develop high tensile stresses, and considering appropriate normal and shear stress-displacement laws for opening/closing and sliding movements [13, 14] (Figure 3).

The joint material elastic properties are the normal stiffness $\mathrm{K_N}$ and shear stiffness $\mathrm{K_T}$, and the strength properties are the cohesion c and friction angle ϕ. In order to evaluate the admissibility of the stress state in a generic point of the joint surface, given by $\underset{\sim}{\sigma} = [\tau_1 \quad \tau_2 \quad \sigma_\mathrm{N}]^\mathrm{T}$, it is convenient to consider the normal stress σ_N and an equivalent positive shear stress value $\tau = \sqrt{\tau_1{}^2 + \tau_2{}^2}$, for comparison with the joint material strength. Based on the Mohr Coulomb criterion, the tensile strength f_t and the shear strength f_t are

$$f_t = c.\frac{2\cos(\phi)}{1+\sin(\phi)}$$
$$\tau_R = c + |\sigma_\mathrm{N}|.\tan(\phi) \tag{11}$$

As seen in the above expressions, the joints resist to opening and sliding movements by friction and cohesion. The resistance to shear forces is also influenced by the normal stress.

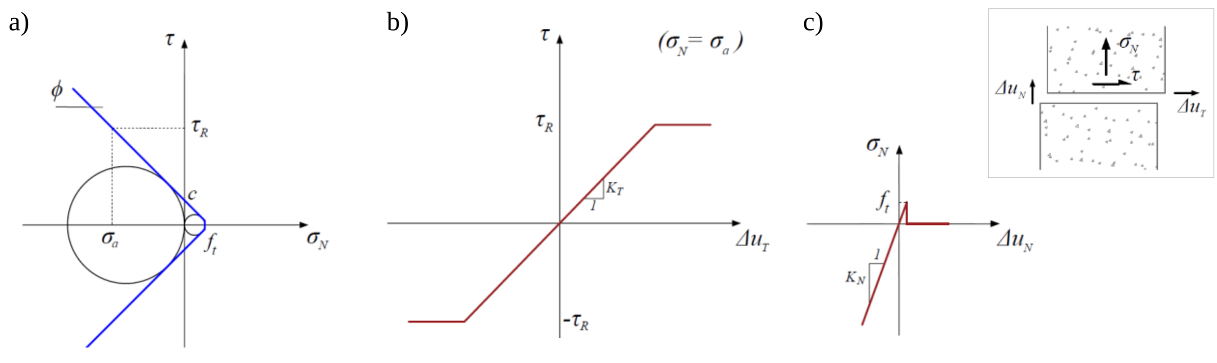

Figure 3. Model used to simulate non-linear joint behaviour (with cohesion): (a) Mohr-Coulomb failure criterion; (b) shear stress-relative displacement law; and (c) normal stress-relative displacement law.

Concrete damage model

The non-linear behaviour of concrete up to failure is simulated using a 3D isotropic constitutive damage model with strain-softening, considering damage under both tension and compression [20,21]. This is a complete model that enables to reproduce crack formation and propagation under tension, and it can also cope with 3D confinement under compression; there are two fundamental features for non-linear analysis of concrete dams, namely under strong earthquakes, since high tensions and compressions may occur.

For a 3D problem, and assuming the internal isotropic damage is defined by the damage variable d, the non-linear constitutive relation is established as $\underset{\sim}{\sigma} = (1-d)\,\underset{\sim}{\tilde{\sigma}}$, where $\underset{\sim}{\tilde{\sigma}} = \underline{D} \cdot \underset{\sim}{\varepsilon}$ is the effective stress tensor. Since the implemented model simulates the non-linear concrete behaviour with strain-softening under both tension and compression, which involve dissimilar features, two independent scalar damage variables are used to characterize the internal damage state, namely: d^+, for damage under tension, and d^-, for damage under compression [21]. Additionally, the effective stress tensor $\underset{\sim}{\tilde{\sigma}}$ is decomposed into the tensile and compressive effective stress tensors, $\underset{\sim}{\tilde{\sigma}}^+$ and $\underset{\sim}{\tilde{\sigma}}^-$, which are represented in the space of the principal stresses and directions. Therefore, the non-linear constitutive law of the described damage model is simply written as

$$\underset{\sim}{\sigma} = (1-d^+)\,\underset{\sim}{\tilde{\sigma}}^+ + (1-d^-)\,\underset{\sim}{\tilde{\sigma}}^- \qquad (12)$$

where the damage variables are always $d^+ \geq 0$ and $d^- \geq 0$, in order to properly represent the irreversible nature of material deterioration; the evolution of the concrete deterioration process is simulated based on specific damage evolution laws, and controlled using appropriate damage criteria [20,21]. The implemented constitutive law enables the calculation of the true stress tensor $\underset{\sim}{\sigma}$ at any material point, knowing the tensile and compressive components of the effective stress tensor and the damage variables that characterize the internal damage state. Examples of stress-strain diagrams obtained with this constitutive damage law are presented in Figure 4 for uniaxial tension and compression, where f_0^+ and f_0^- indicate the maximum admissible tension and compression for linear elastic behaviour, while f_t and f_c are the peak tensile and compressive stresses.

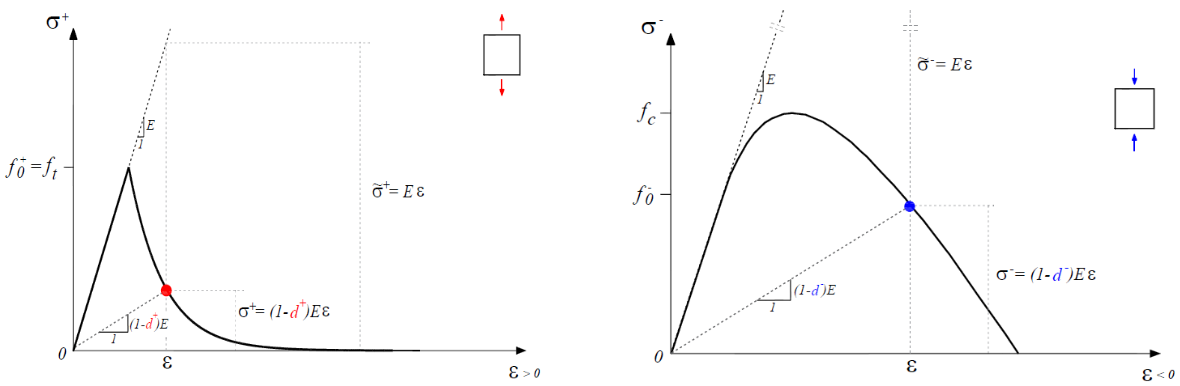

Figure 4. Constitutive damage model with two independent damage variables for concrete: stress-strain diagrams for uniaxial tension and compression.

4. CASE STUDY 1: CABRIL DAM, PORTUGAL

4.1. Dam description

Cabril dam is a 132 m high double curvature arch dam, with a 290 m long crest (Figure 5). This is the highest dam in Portugal, and it has been in operation since 1954 on the Zêzere River. The maximum thickness is of 20 m at the base, and the minimum is of 4.5 m, at an elevation around 7 m below the crest. The dam is built on a granite mass rock foundation of good quality. During the first filing of the reservoir, horizontal cracks appeared in the upper part of the dam, around el. 280 m to el. 290 m: according to several computational studies, this occurred due to structural effects associated with the larger thickness of the dam crest; nevertheless, multiple analyses showed the cracks do not affect dam performance [22].

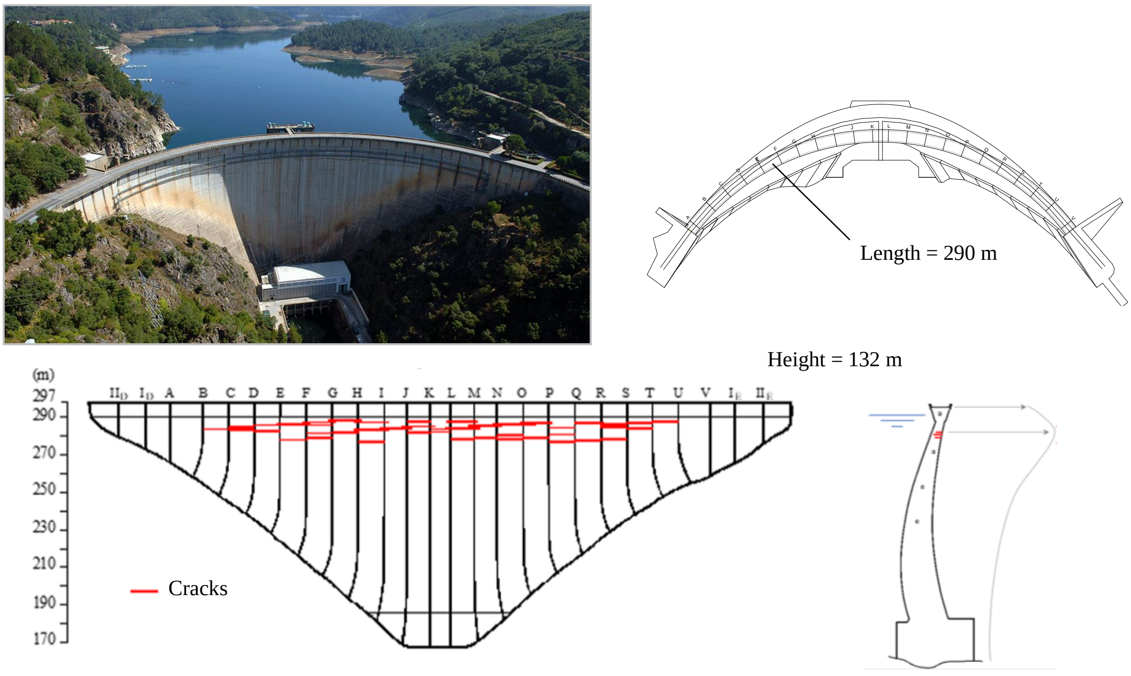

Figure 5. Cabril dam, Portugal. Aerial view and technical drawings.

4.2. Finite element model and load combination

The finite element simulations for Cabril dam were carried out using the model of the dam-reservoir-foundation system presented in Figure 6. The discretization was defined in order to have three elements in thickness in the dam body. The dam concrete and foundation rock are isotropic materials, considering Young's modulus E = 25 GPa and Poisson's ratio $\nu = 0.2$. The water in the reservoir is a compressible fluid with a pressure wave propagation velocity $c_w = 1440$ m/s (mean reservoir water temperature around 15ºC). The adopted material properties have been validated in previous studies, based on experimental results from vibrations monitoring data [22].

For linear seismic analysis, a version of the model without joints is used and linear-elastic behaviour of concrete is considered. On the other hand, for non-linear seismic analysis [17], all vertical contraction joints are incorporated into the model, considering appropriate normal and shear stiffness values, null cohesion and a 30º friction angle. The existing cracking band in the dam is considered in a simplified way by introducing a single horizontal crack, using interface elements at el. 285 m; higher stiffness values are considered, to limit the crack opening movements (expected scenario for higher reservoir water levels). The non-linear behaviour of concrete up to failure is simulated using a strain-softening constitutive damage law, assuming tensile strength $f_t = 3\,\text{MPa}$ and compressive strength $f_c = -30\,\text{MPa}$.

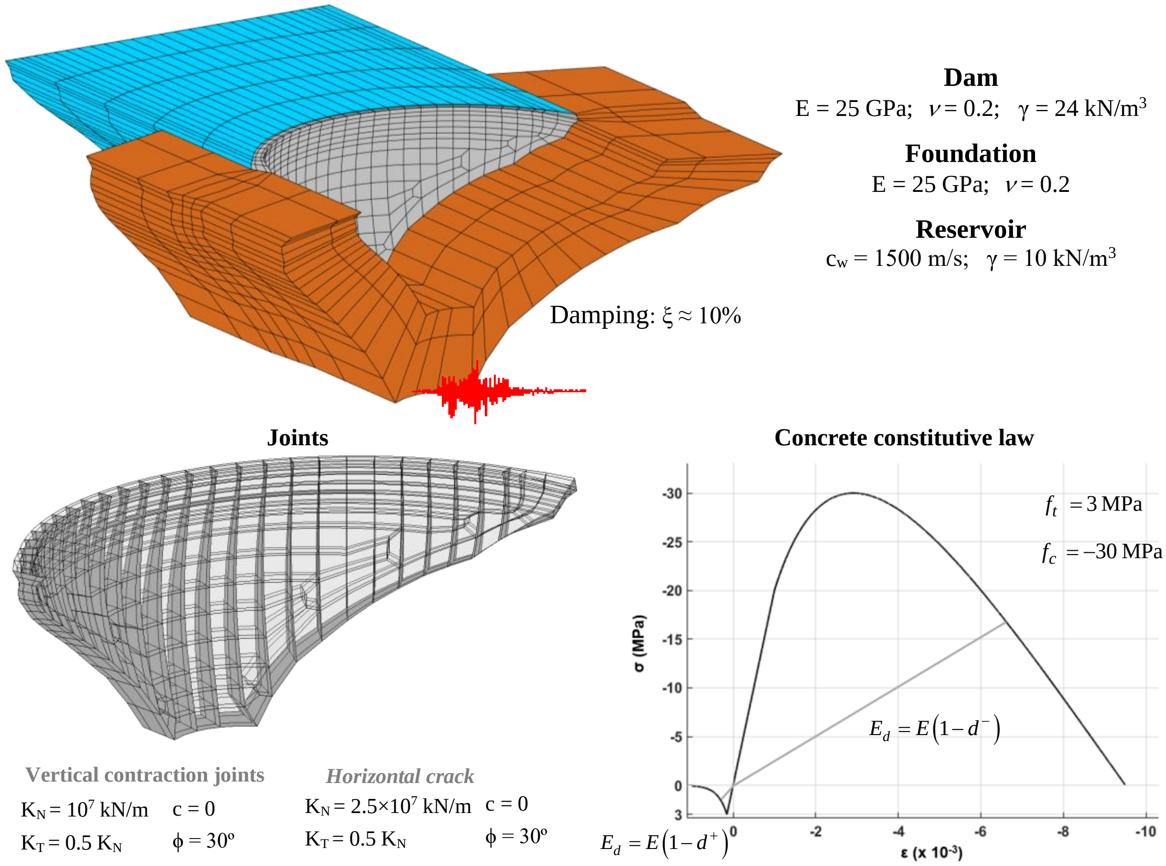

Figure 6. Model of the dam-reservoir-foundation system used for seismic analysis of Cabril dam. Material properties, dam mesh with joints, concrete constitutive law.

The applied load combination (Figure 7) includes the self-weight of the dam (SW), the hydrostatic pressure for full reservoir (HP297), and a seismic load applied in the upstream-downstream direction (SEISMICL). For this study, the seismic input is an artificial intensifying acceleration time history, designed for Endurance Time Analysis (ETA) and provided in [23], with peak accelerations increasing up to 1g in 10 s.

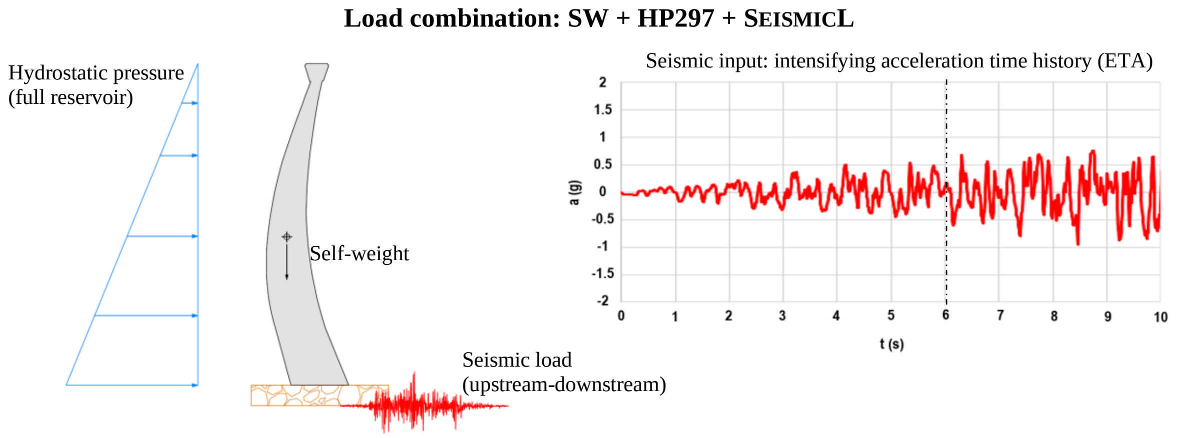

Figure 7. Load combination for seismic analysis of Cabril dam and seismic input.

4.3. Linear and non-linear seismic response

The seismic response of Cabril dam under the load combination SW + HP297 + SEISMICL is analysed next. The seismic calculations were performed up to 6 seconds of the intensifying acceleration time history, which gives a peak ground acceleration of approximately 0.55g.

The results computed in the linear analysis are compared with those calculated using the non-linear model, considering joint movements and concrete damage. The comparative study is focused on time instants in which the dam experiences important deformations in the upstream direction, in order to evaluate the influence of the joint movements in the structural response (when the dam moves towards downstream, it is mainly under compressive stresses and the vertical joints close).

Starting with the linear seismic response (Figure 8), in the captured instant the maximum displacements (≈ 75 mm) are computed at the crest of the central cantilevers. As for the corresponding principal stresses fields, the higher arch tensions (8MPa) arise at the top of the central cantilevers, on the upstream face. Important tensions also occur at the base of the shorter lateral cantilevers (4 MPa), on the upstream surface, and at the upper part of the lateral cantilevers (from 3 and 4.9 MPa), near the downstream face.

As for the non-linear seismic response (Figure 9), when the dam moves in the upstream direction the vertical contraction joints tend to open. In this case, the larger upstream displacements are now calculated along the top of the taller cantilevers of dam, particularly at the top of the lateral cantilevers (163.9 mm), where the larger joint opening (≈ 10 mm) and sliding (≈ 20 mm) movements occur.

Regarding the non-linear stresses, it is possible to see that the opening/sliding of the vertical contraction joints resulted in a reduction of the arch effect, and therefore in a release of the arch tensions along the upper part of the dam; this prevented the occurrence of concrete tensile damage. The stress redistribution process that followed led to an increase of the vertical stresses, both of vertical compressions at the upstream face and of tensions at the downstream face. However, the vertical tensions were released due to non-linear concrete behaviour under tension, as tensile damage progressed, namely along the upper half of the taller cantilevers and over the entire height of shorter cantilevers, on the downstream face. High tensile damage values also occurred near the upstream base, along the insertion. In several zones the tensile damage values reached the maximum damage value (d^+=100%), indicating that concrete failure has occurred. Nevertheless, in the conducted seismic simulation there was no compressive damage.

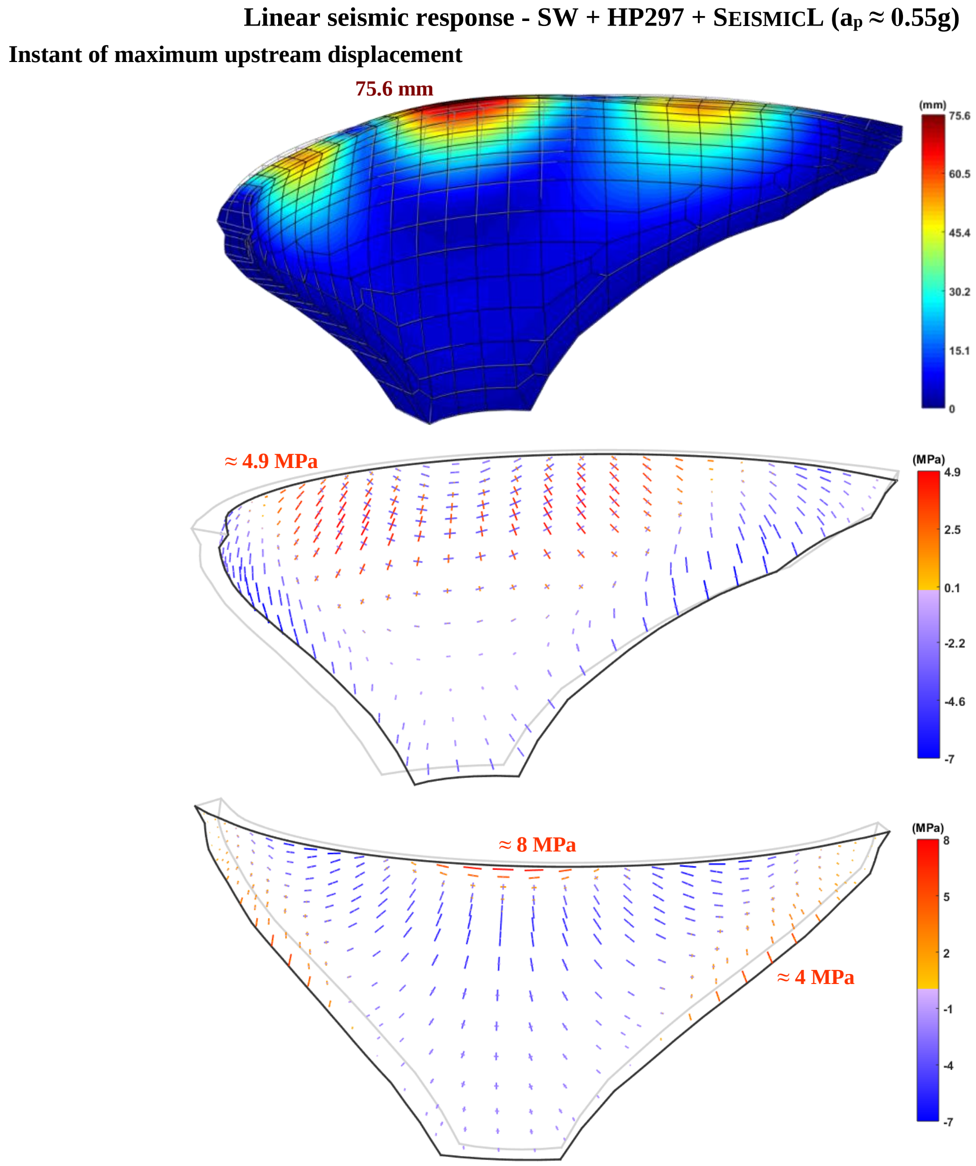

Figure 8. Linear seismic response of Cabril dam for SW+HP297+SEISMICL. Deformed shapes and principal stresses (upstream and downstream view).

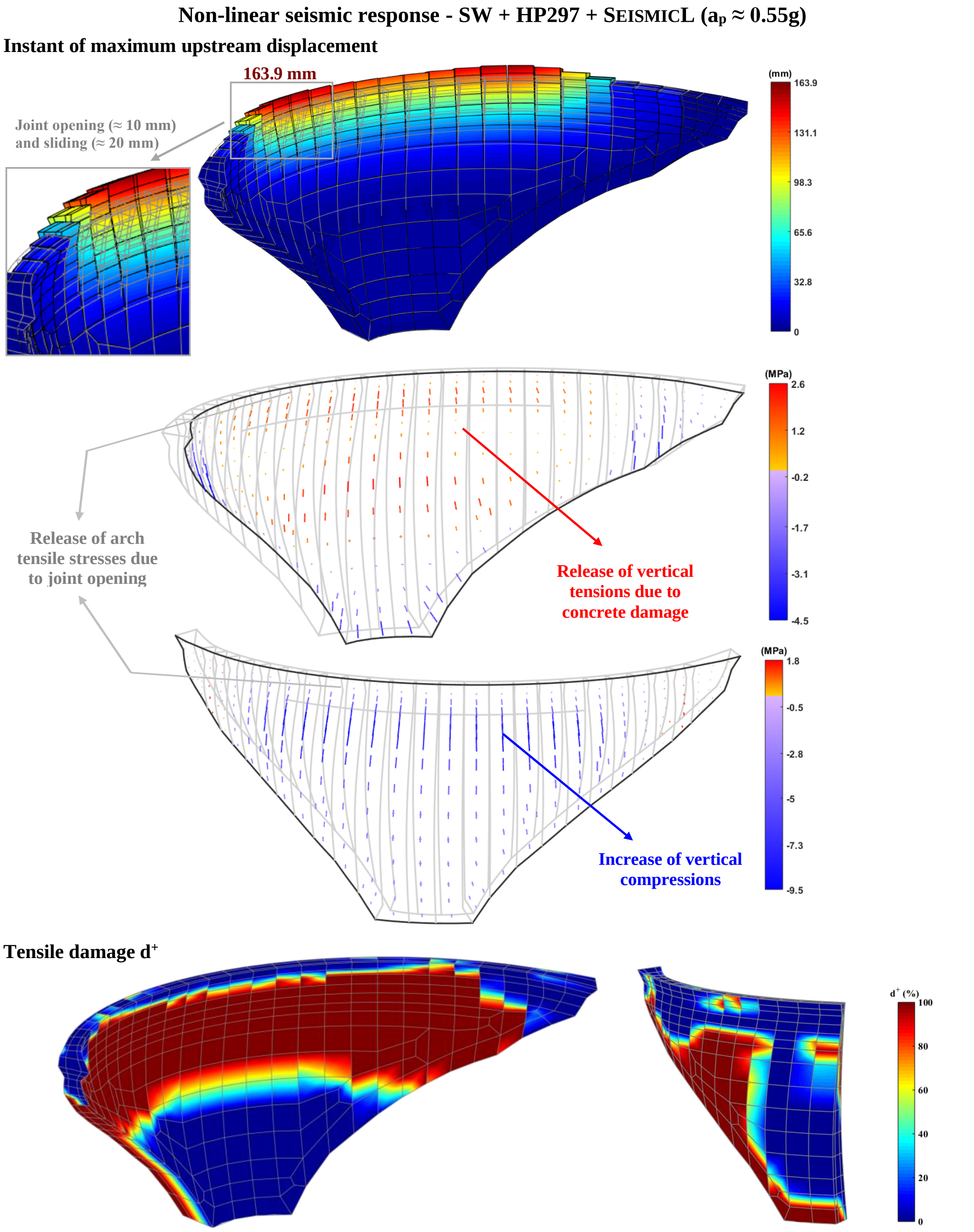

Figure 9. Non-linear seismic response of Cabril dam for SW+HP297+SEISMICL. Deformed shapes, principal stresses (upstream and downstream view), and tensile damage.

5. CASE STUDY 2: CAHORA BASSA DAM, MOZAMBIQUE

5.1. Dam description

Cahora Bassa dam is a thin double curvature arch structure, with a maximum height of 170 m and a crest length of 303 m (Figure 10). The thickness of the central section goes from 23 m at the base, to around 4 m at the crest, which presents a unique half-hollow geometry. Cahora Bassa dam entered in operation in 1974 on the Zambezi River, in western Mozambique, and it is one of the largest dams in Africa. A concrete swelling phenomenon was detected in Cahora Bassa dam in the 1980s, which is evidenced by a typical cracking pattern that can be seen at the crest. This dam was constructed on a gneissic granite rock mass of very good quality.

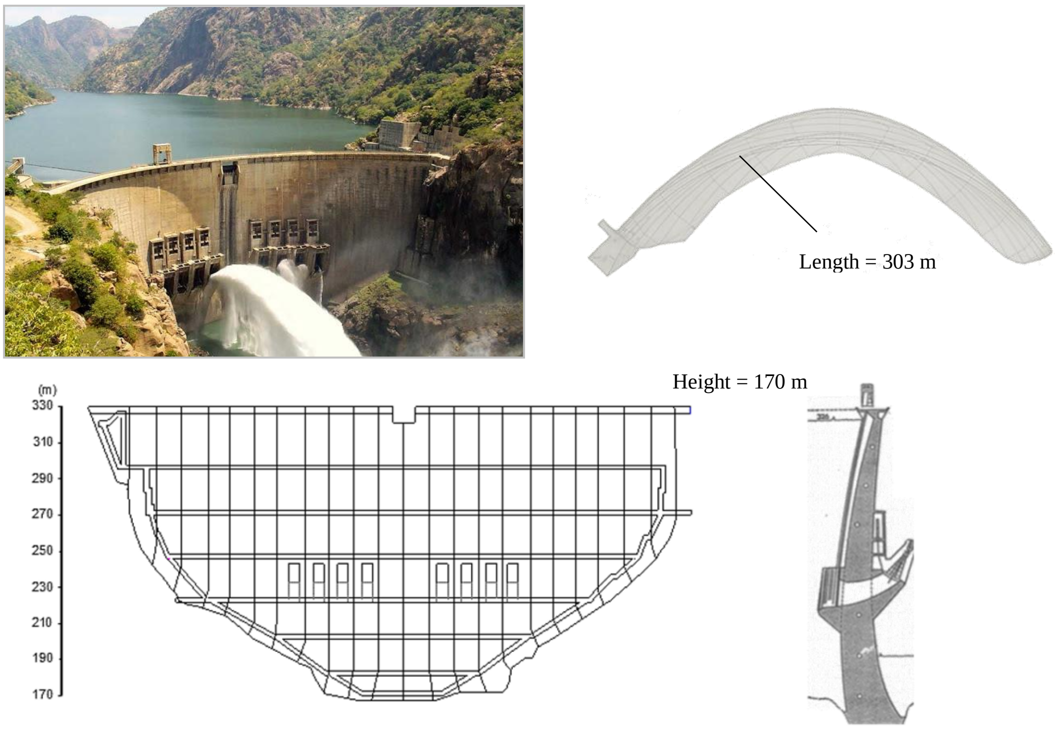

Figure 10. Cahora Bassa dam, Mozambique. Aerial view and technical drawings.

5.2. Finite element model and load combination

The numerical calculations were performed using the model of the Cahora Bassa dam-reservoir-foundation system in Figure 11, with three elements in thickness in the dam body (the half-hollow crest shape and the geometry of the spillways are simulated in a simplified way). The dam concrete and the foundation rock materials are assumed to be isotropic materials, using Young's modulus E = 40 GPa and Poisson's ratio ν = 0.2, while the reservoir water is considered a compressible fluid with a pressure wave propagation velocity c_w = 1500 m/s (considering the mean reservoir water temperature at 25ºC). The material properties have been calibrated in previous studies using dynamic experimental data [22].

The linear seismic calculation was conducted using a version of the model without joints and assuming linear-elastic concrete behaviour. The non-linear seismic simulation was carried out using the model with all vertical contraction joints and considering a constitutive damage law to simulate the behaviour of concrete up to failure under tension and compression [17].

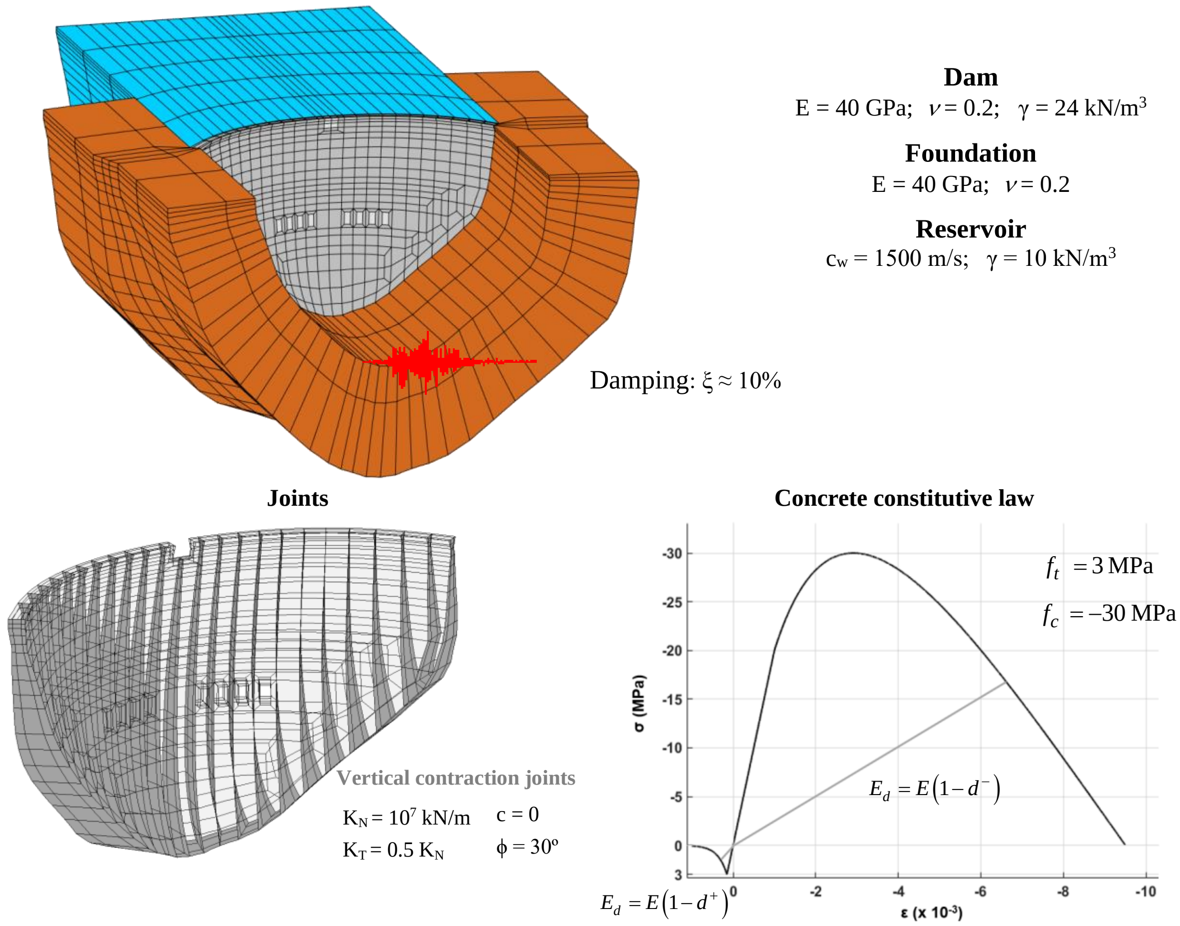

Figure 11. Model of the dam-reservoir-foundation system used for seismic analysis of Cahora Bassa dam. Material properties, dam mesh with joints, concrete constitutive law.

As in the previous case study, the load combination (Figure 12) includes the dam self-weight (SW), the hydrostatic pressure for a full reservoir-condition (HP331), and the intensifying seismic action applied in the upstream-downstream direction (SEISMICL).

5.3 Linear and non-linear seismic response

The seismic behaviour of Cahora Bassa under a strong earthquake is analysed next, considering the load combination SW + HP331 + SEISMICL. The seismic simulation was conducted up to 6 seconds of the acceleration time history, which corresponds to a peak ground acceleration of about 0.55g. The results from linear seismic response and non-linear seismic response are compared, with emphasis on the deformed shapes and principal stresses for the time instants in which the dam moves towards upstream, with a view to analyse the structural effects due to the joint movements and the resulting concrete tensile damage.

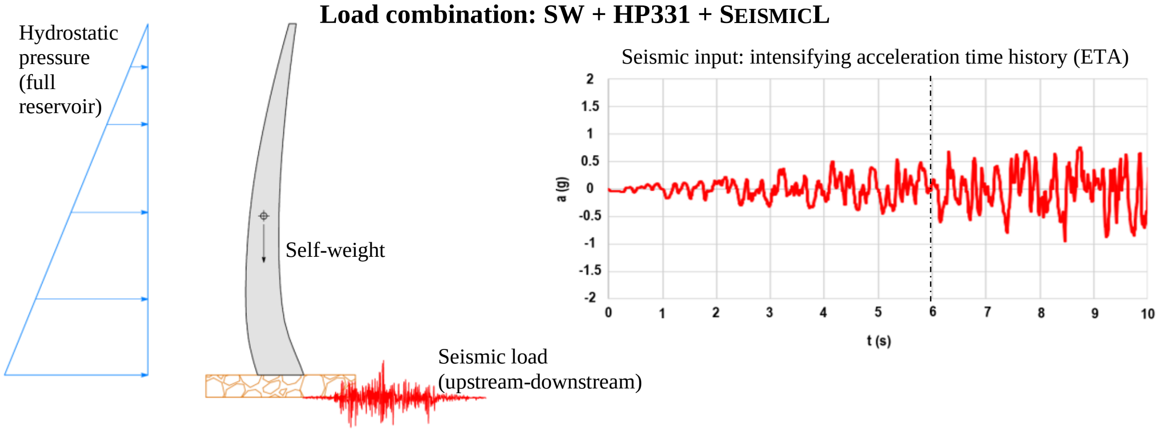

Figure 12. Load combination for seismic analysis of Cahora Bassa dam and seismic input.

Starting with the linear seismic response (Figure 13), the maximum displacements (≈ 97 mm) are computed at the crest of the lateral cantilevers, located halfway between the central section and the abutments. Regarding the fields of principal stresses, very high arch tensions, between 15 to 20 MPa, arise in the central upper part of the dam, around the surface spillway, at the downstream face, and near the crest of the lateral cantilevers, at the upstream face.

In what concerns the non-linear seismic response (Figure 14), as the dam moves towards upstream the vertical contraction joints open, resulting in an increase of the maximum displacements at the top of the lateral cantilevers (117.5 mm), where the larger joint openings occur (≈13 mm). In the captured instant, the global displacement amplitude in the upstream-downstream direction between the central cantilevers, which move towards downstream, and the lateral cantilevers, which move in the upstream direction, is far greater in the non-linear model (≈ 210 mm) than in the linear model (≈ 120 mm).

As for the non-linear stresses, the results show that the opening of the vertical contraction joints led to a reduction of the arch effect, and thus to a release of the arch tensions along the top of the dam; as seen in the previous case study, this avoided the occurrence of tensile damage along the upper blocks. The subsequent stress redistribution caused an increase of the vertical compressions at upstream face and of the vertical tensions at the downstream face. These vertical tensions were released as tensile damage expanded along the upper half of most of the dam cantilevers (downstream face). Tensile damage also occurred at the upper part of the upstream face of several lateral cantilevers, and along the upstream base, caused by tensions oriented in the normal direction to the insertion (which arise when the dam moves towards downstream). Moreover, due to the dam asymmetry, tensile damage is also noticeable at the top of the left-most cantilever, near the abutment, due to high arch tensions. Finally, it is worth highlighting there was no compressive damage in Cahora Bassa dam.

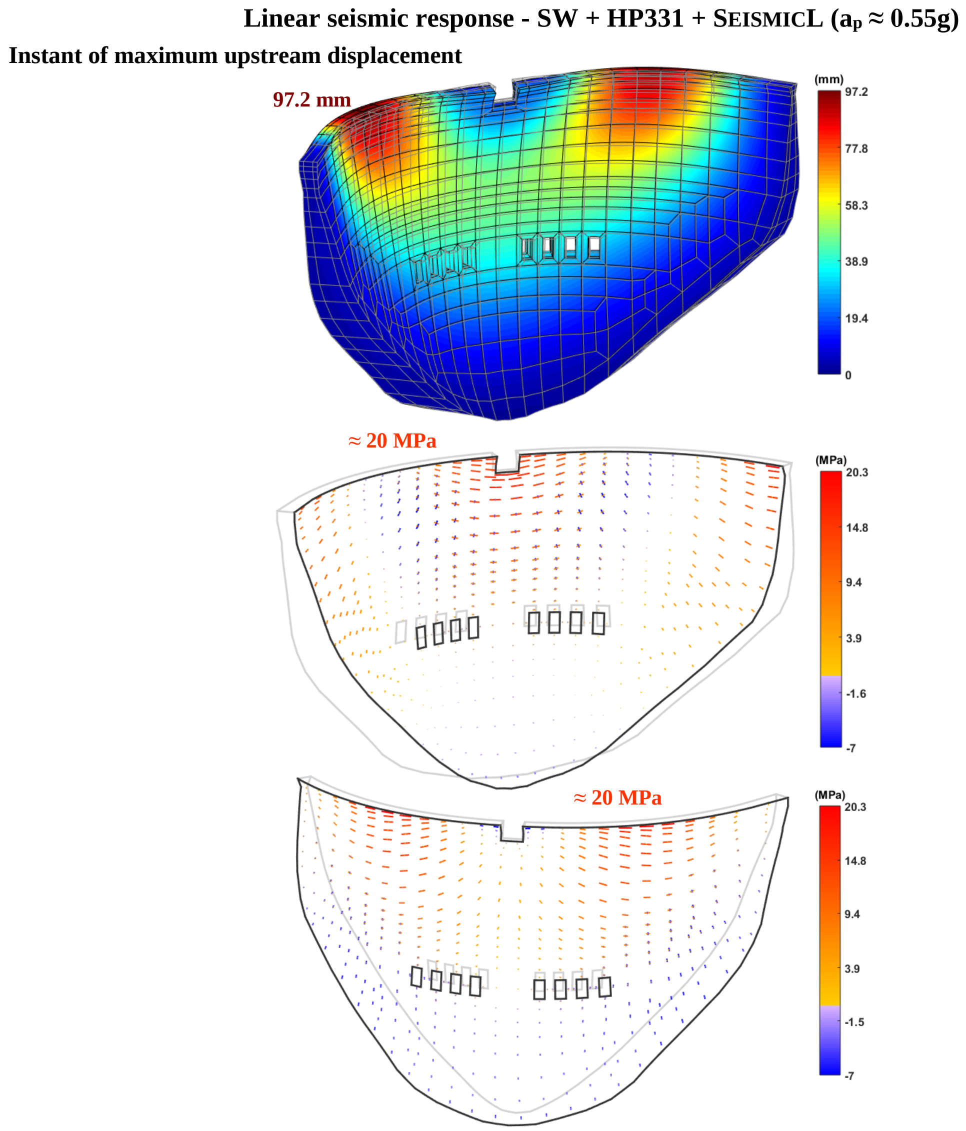

Figure 13. Linear seismic response of Cahora Bassa dam for +HP331+SEISMICL. Deformed shapes and principal stresses (upstream and downstream view).

6. CONCLUSIONS

This paper was focused on numerical modelling the seismic behaviour of arch dams under strong earthquakes. The finite element program *DamDySSA*, developed for dynamic analysis of concrete dams, was presented. Emphasis was given to the implemented numerical methods, based on a couped approach to solve the dynamic equation of the dam-reservoir-foundation system, including: (i) a time-stepping method for linear seismic analysis; and (ii) a combined time-stepping and stress-transfer method for non-linear seismic analysis, using a joint constitutive model to simulate opening/closing and sliding movements and a constitutive damage model to reproduce damage under tension and compression.

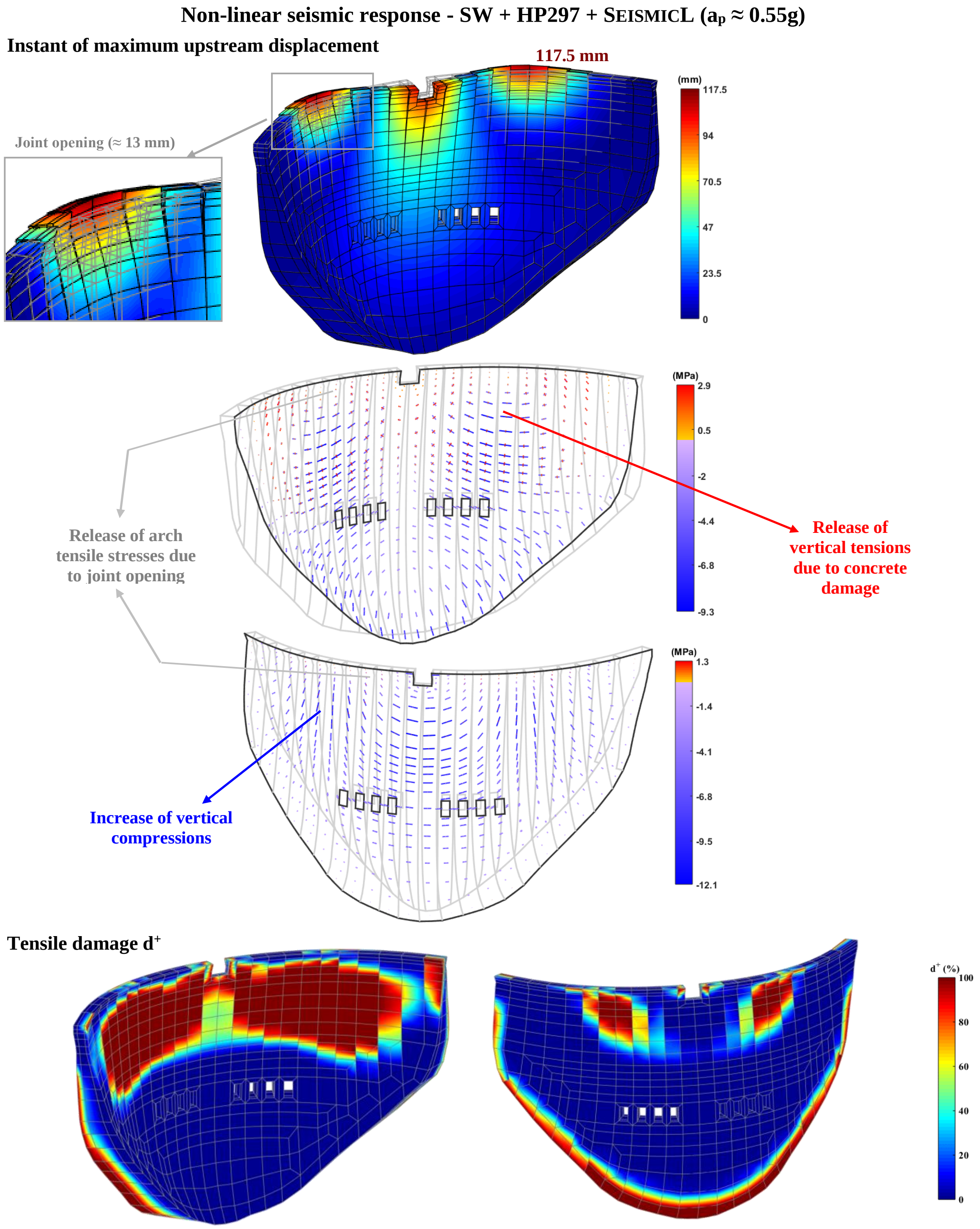

Figure 14. Non-linear seismic response of Cahora Bassa dam for SW+HP331+SEISMICL. Deformed shapes, principal stresses (upstream and downstream view), and tensile damage.

The program was used for seismic response analysis of two double curvature arch dams, namely the 132-m high Cabril dam (Portugal), and the 170 m-high Cahora Bassa dam (Mozambique), considering a load combination including the dam self-weight, the hydrostatic pressure (full reservoir), and a seismic action represented by an intensifying acceleration time history. The linear and non-linear seismic response results (for peak ground acceleration up to around 0.55g) were compared to investigate the effects of the joint movements on the dam structural behaviour: overall, the study of these two arch dams demonstrated that the opening of the vertical contraction joints resulted in a release of arch tensile stresses at the top of the dam, and thus in an increase of vertical stresses along the height of the cantilevers. The resulting vertical tensions ended up surpassing concrete tensile strength in multiple locations, hence causing high concrete tensile damage.

This work enabled to show the potential of the implemented methods and thus of *DamDySSA* for conducting behaviour prediction studies of arch dams, including linear and non-linear seismic analysis. only for linear seismic analysis, but also for non-linear seismic analysis. Furthermore, since the non-linear model enables to combine the effects due to joint movements and the tensile and compressive concrete damage, this program can be of great value for supporting seismic design and safety assessment of large arch dams.

ACKNOWLEDGEMNTS

The authors wish to express their gratitude to Eletricidade de Portugal (EDP) and Hidroeléctrica de Cahora Bassa (HCB), as well as to the Portuguese Foundation for Science and Technology (FCT) for funding the Project "Seismic and Structural Health Monitoring for Large Concrete Dams (SSHM4Dams)", PTDC / ECI-EGC / 5332/2020.

REFERENCES

[1] ICOLD. *Bulletin 158: Dam surveillance guide.* (2019).

[2] M. Wieland, *Seismic Hazard and Seismic Design and Safety Aspects of Large Dam Projects*. in *Perspectives on European Earthquake Engineering and Seismology. Geotechnical, Geological and Earthquake Engineering*, A. Ansal (ed.). Springer, Cham, pp. 627–650, (2014).

[3] IJHD, World Atlas & Industry Guide. *International Journal of Hydropower and Dams*. Aqua Media Int. Ltd., (2021).

[4] S. Oliveira, A. Alegre, E. Carvalho, P. Mendes, and J. Proença, Seismic and structural health monitoring systems for large dams: theoretical, computational and practical innovations. *Bulletin of Earthquake Engineering*, (2022).

[5] A. K. Chopra, Earthquake Analysis of Arch Dams: Factors to Be Considered. *Journal of Structural Engineering*, vol. 138, no. 2, pp. 205–214, (2012).

[6] H. M. Westergaard, Water pressures on dams during earthquakes. *Transactions (ASCE)*, vol. 98, pp. 418–472, (1933).

[7] O. C. Zienkiewicz and P. Bettess, Fluid-structure dynamic interaction and wave forces. An introduction to numerical treatment. *International Journal on Numerical Methods in Engineering*, vol. 13, pp. 1–16, (1978).

[8] R. W. Clough, Non-linear mechanisms in the seismic response of arch dams.

International Research Conference on Earthquake Engineering, Skopje, Yugoslavia, (1980).

[9] R. B. Reimer, *Deconvolution of seismic response for linear systems*. Report No. EERC 73-10. University of California, Berkeley, (1973).

[10] Z. Chuhan, J. Feng, and O. A. Pekau, Time domain procedure of FE-BE-IBE coupling for seismic interaction of arch dams and canyons. *Earthquake Engineering & Structural Dynamics*, vol. 24, no. 12, pp. 1651–1666, (1995).

[11] A. Alegre, E. Carvalho, B. Matsinhe, P. Mendes, S. Oliveira, and J. Proença, Monitoring vibrations in large dams. *HYDRO 2019*, Porto, Portugal, (2019).

[12] E. Robbe, Seismic back analysis of Monticello arch dam - blind prediction workshop and additional analyses. *USSD 2017 Annual Conference and Exhibition*, Anaheim, California, (2017).

[13] G. L. Fenves, S. Mojtahedi, and R. B. Reimer, Effect of contraction joints on earthquake response of an arch dam. *Journal of Structural Engineering (ASCE),* vol. 118, pp. 1039–1055, (1992).

[14] A. Niwa and R. W. Clough, Non-linear seismic response of arch dams. *Earthquake Engineering and Structural Dynamics*, vol. 10, pp. 267–281, (1982).

[15] M. Cervera, J. Oliver, and R. Faria, Seismic evaluation of concrete dams via continuum damage models. *Earthquake Engineering & Structural Dynamic*s, vol. 24, no. 9, pp. 1225–1245, (1995).

[16] S. Valliappan, M. Yazdchi, and N. Khalili, Seismic analysis of arch dams - a continuum damage mechanics approach. *International Journal of Numerical Methods in Engineering*, vol. 45, no. 11, pp. 1695–724, (1999).

[17] A. Alegre, Modelling and monitoring the dynamic behaviour of concrete dams. Modal analysis and seismic response, PhD Thesis, Instituto Superior Técnico (University of Lisbon), Portugal, (2021).

[18] O. C. Zienkiewicz, R. L. Taylor, and J. Z. Zhu, *The Finite Element Method: Its Basis and Fundamentals*. 7^{th} ed. Elsevier Butterworth-Heinemann, (2013).

[19] O. C. Zienkiewicz, R. L. Taylor, and D. D. Fox, *The Finite Element Method for Solid and Structural Mechanics*. 7^{th} ed. Elsevier, 2014.

[20] S. Oliveira and R. Faria, Numerical simulation of collapse scenarios in reduced scale tests of arch dams. *Engineering Structures*, vol. 28, no. 10, pp.1430–1439, (2006).

[21] S. Oliveira, Modelos para análise do comportamento de barragens de betão considerando a fissuração e os efeitos do tempo. Formulações de dano. PhD Thesis, University of Porto (FEUP), (2000).

[22] A. Alegre, S. Oliveira, E. Carvalho, P. Mendes, J. Proença, and B. Matsinhe, Continuous dynamic monitoring of large arch dams and vibration-based damage detection. *HYDRO 2022*, Strasbourg, France, (2022).

[23] J. Salamon, M. A. Hariri-Ardebili, R. Malm, C. Wood, and G. Faggiani, Numerical Analysis of Dams. Theme A: Seismic Analysis of Pine Flat Concrete Dam, in *15th ICOLD International Benchmark Workshop*, vol. 91, Milan, Italy, (2021).